Revista EIA
ISSN: 1794-1237
revista@eia.edu.co
Escuela de Ingeniería de Antioquia
Colombia

Bejarano Gaitán, Gilberto; Echavarría García, Aida Milena; Quirama Ossa, Alix Caterine; Osorio Vélez, Jaime Alberto

DEPOSITION AND PROPERTIES CHARACTERISATION OF TaN COATINGS DEPOSITED AT DIFFERENT NITROGEN CONTENTS

Revista EIA, vol. 13, núm. 25, enero-junio, 2016, pp. 69-80
Escuela de Ingeniería de Antioquia
Envigado, Colombia

Revista EIA, ISSN 1794-1237 / Año XIII / Volumen 13 / Edición N.25 / Enero-Junio 2016 / pp. 69-80
Publicación semestral de carácter técnico-científico / Universidad EIA, Envigado (Colombia)

DEPOSITION AND PROPERTIES CHARACTERISATION OF TaN COATINGS DEPOSITED AT DIFFERENT NITROGEN CONTENTS

Gilberto Bejarano Gaitán[1]
Aida Milena Echavarría García[1]
Alix Caterine Quirama Ossa[1]
Jaime Alberto Osorio Vélez[2]

ABSTRACT

This work focused on the study of the influence of nitrogen content on the microstructure, chemical composition, mechanical and tribological properties of TaN coatings deposited on 420 stainless steel and silicon samples (100) using the magnetron sputtering technique. For the deposition of the TaN coatings an argon/nitrogen atmosphere was used, varying the flux of nitrogen between 12% and 25%. For coating's characterization, Scanning electron microscopy, Energy dispersive X-ray spectroscopy, Atomic force microscopy, X-Ray diffraction, Microraman spectroscopy, Micro-hardness tester and a ball on disc tribometer were used. A refining of the columnar structure of the coatings, accompanied by a decrease in their thickness with the increased nitrogen content was observed. Initially, fcc-TaN (111) cubic phase growth was observed, this phase was changed to the fcc-TaN (200) above N_2 12%. For contents greater than N_2 18%, another nitrogen-rich phase was formed and the system tended to amorphicity, particularly for coating with N_2 25% content. TaN-1 sample deposited with N_2 12% in the gas mixture presented the highest micro-hardness value of 21.3GPa and the lowest friction coefficient and wear rate of 0.02 and $1.82x10^{-7}$ (mm^3/Nm), respectively. From the obtained results, an important relationship between the microstructural, mechanical and tribological properties of the coated samples and their nitrogen content was observed.

KEYWORDS: Hard Coatings; Magnetron Sputtering; Tantalum Nitride; Surface Modification; Wear resistance; Tribology.

DEPOSICIÓN Y CARACTERIZACIÓN DE LAS PROPIEDADES DE RECUBRIMIENTOS DE TaN DEPOSITADOS CON DIFERENTES CONTENIDOS DE NITRÓGENO

RESUMEN

Este trabajo se enfocó en el estudio de la influencia del contenido de nitrógeno sobre la microestructura, composición química, propiedades mecánicas y tribológicas de los recubrimientos de TaN depositados sobre acero inoxidable

[1] Centro de Investigación Innovación y Desarrollo de Materiales – CIDEMAT, Universidad de Antioquia-UdeA, Medellín – Colombia.
[2] Grupo de Estado Sólido – Instituto de Física, Universidad de Antioquia-UdeA, Medellín – Colombia

Autor de correspondencia: Bejarano-Gaitán, G. (Gilberto). Calle 60 75-150, Apto 821, Ribera del Valle, Medellín, Colombia / Tel.; (4)4462883
Correo electrónico: gilberto.bejarano@udea.edu.co

Historia del artículo:
Artículo recibido: 28-IV-2015 / Aprobado: 06-IV-2016
Disponible online: 30 de octubre de 2016
Discusión abierta hasta octubre de 2017

DOI: http:/dx.doi.org/10.14508/reia.2016.13.25.69-80

420 y silicio (100) mediante la pulverización catódica. Los recubrimientos se depositaron en una atmosfera de argón/ nitrógeno variando el flujo de nitrógeno entre 12% y 25%, y fueron caracterizados por SEM, EDX, DRX, AFM, Microraman, Microindentación y usando un tribómetro tipo bola sobre disco. Se apreció una refinación de la estructura columnar de los recubrimientos acompañado de una disminución de su espesor con el incremento del contenido de nitrógeno en éstos. Inicialmente se observó un crecimiento preferencial de la fase cúbica fcc del TaN (111), la cual cambió a la estructura fcc TaN (200) por encima del 12% de N_2. A contenidos mayores al 18% de N_2 se forman otras fases ricas en nitrógeno y el sistema tiende a la amorficidad, muy particularmente para un 25% de N_2. El recubrimiento TaN-1, depositado con 12% N_2 en la mezcla de gases, presentó la mayor dureza de 21.3 GPa, el menor coeficiente de fricción y tasa de desgaste de 0,02 y $1{,}82x10^{-7}$ (mm^3/Nm), respectivamente. A partir de los resultados obtenidos se observó una importante relación entre la microestructura, las propiedades mecánicas y tribológicas de las muestras recubiertas y su contenido de nitrógeno.

PALABRAS CLAVE: recubrimientos duros; pulverización catódica; nitruro de Tantalio; modificación superficial; resistencia al desgaste; tribología.

DEPOSIÇÃO E CARACTERIZAÇÃO DAS PROPRIEDADES REVESTIMENTOS DEPOSITADOS TaN COM DIFERENTES CONTEÚDOS DE AZOTO

RESUMO

Este trabalho centrou-se em estudar a influência do teor de azoto sobre a microestrutura, composição química, propriedades mecânicas e tribológicas dos revestimentos depositados TaN em aço inoxidável 420 e de silício (100) por pulverização catódica. Os revestimentos foram depositados em árgon / azoto variando o fluxo de azoto entre 12% e 25%, e foram caracterizados por SEM, EDX, DRX, AFM, microRaman, microindentation e escreva tribômetro usando uma bola no disco. um aperfeiçoamento de revestimentos de estrutura colunar acompanhada por uma diminuição da espessura com o aumento do teor de azoto nestes apreciado. Inicialmente observou-se um crescimento preferencial da fase cúbica do tan FCC (111), que mudou a estrutura FCC castanho-amarelado (200) acima de 12% de N2. A teores superiores a 18% de N2 outras fases ricos em azoto são formados e o sistema tende a amorficidade, muito particularmente de 25% de N2. O revestimento de TAN-1, depositado com 12% de N2 na mistura de gás, teve o maior dureza de 21,3 GPa, um coeficiente de atrito mais baixo e taxa de desgaste de 0,02 1,82x10-7 (mm3 / Nm) respectivamente. A partir dos resultados de uma relação importante entre a microestrutura, observou-se propriedades mecânicas e tribológicas das amostras revestidas e o seu teor de azoto.

PALAVRAS-CHAVE: duro Revestimentos, pulverização catódica, tântalo nitreto, modificação da superfície, resistência ao desgaste, Tribologia

1. INTRODUCTION

The superficial modification of metallic materials with different coatings to improve their performance is one of the disciplines that are being investigated in a vertiginous way. Tantalum nitride is a material characterized by high hardness, corrosion resistance, chemical and thermal stability, which makes it very attractive for applications such as integrated circuits, diffusion barriers for cooper-base metallization and resistors, as well as in form of hard coating for cutting and forming tools and machine parts.(Riekkinen *et al*. 2002; Bromark *et al*. 1997).

However, other application fields are promising for this material, such as bioengineering and materials science, which refers tantalum nitride as biocompatible, whose features obtained from its manufacturing process can achieve porous structures (closed or interconnected), that can be favorably used in applications such as medical implants, where direct contact with bone structures is required, since its elastic modulus is very similar to such structures (Pino, 2008). The application's field for tantalum nitride coatings is strongly linked to its microstructure, chemical composition, mechanical and physicochemical properties, which in turn depend, among other facts, on the nitrogen content and on the Ta/N ratio of the coatings. In this work, the influence of nitrogen content on the microstructural and chemical properties, as well as on the mechanical and tribological behavior of the TaN coatings was determined. The obtained and discussed results represent an important database for future researches and are helpful to determine the deposition process parameter of TaN coatings for an appropriated application. Stainless steel 420 was chosen as substrate because the future applications of this coated metal are directed to surgical and dental instrumentation, which are usually manufactured with this steel. However, TaN coatings may be used in applications where high hardness and high wear and corrosion resistance is required, such as cutting and forming tools, extrusion dies, injection molds, discs and cutting blades, drills and end mills, among others. The single crystal silicon substrates were used, as they are very suitable for spectroscopic and X- ray diffraction characterization of the coatings, since the negative influence of the elements of steel is obviated.

2. EXPERIMENTAL DETAILS

2.1. Coatings deposition

TaN coatings were developed using the unbalanced magnetron sputtering technique on Si (100) and 420 stainless steel substrates, which were grounded with silicon carbide abrasive of 350 to 1200 grit sizes, and finally polished with an alumina powder suspension to a mirror finish with an average roughness of Ra= of 0.05 μm, as measured with an optical profilometer. Thereafter, the samples were degreased in an ultrasonic bath with propanol and acetone and then dried using pressured air. Both propanol and acetone were used because when cleaning the samples only with propanol, they came out stained that was avoided by adding acetone. Before deposition of the coatings, an ionic cleaning of the substrates and Ta target (99.9% high-purity) was carried out into the vacuum chamber at a temperature of 100°C during 15 minutes. After this, the TaN coatings were deposited varying the nitrogen gas flow between 8 and 20 sccm while the argon gas flow was maintained constant at 40 sccm, resulting in a percentage chance of nitrogen gas flow in the $N_2/(Ar+N_2)$ gas mixture between 12% and 25%, as indicated in **Table 1**. The gas flow was determined by a mass flow controller GFC17S from Aalborg. Other important process parameter were selected as follows: total time for each process 4 hours, temperature of 120°C, Ta target power 1,500W, bias voltage of substrates (-50V) and process pressure of $6.3x10^{-3}$mbar. The samples were rotated at 20 rpm and located at a distance of 80 mm to the target. Before deposition of each TaN coating system, a Ta interlayer with a thickness of about 100nm was deposited on the samples surfaces.

TABLE 1. NITROGEN CONTENTS IN THE GAS MIXTURES FOR THE DEPOSITED TAN COATINGS BY CONSTANT AR FLOW OF 40 SCCM.

Sample	N2 gas flow (sccm)	$N_2/(Ar+N_2)$
TaN-1	8	12%
TaN- 2	10	14%
TaN- 3	13	18%
TaN- 4	15	20%
TaN- 5	20	25%

2.2. Coatings Characterization

The cross section morphology and the thickness of the coatings, calculated as the average of 3 measurements, were evaluated in a JEOL JSM-

6490LV scanning electron microscope (SEM), while the chemical composition (weight % sigma between 1.06-1.18) was determined by energy dispersive X-rayspectroscopy (EDX) and INCA energy software. The phases composition was characterized with a Panalytical Empyrean X- ray diffractometer using a Cu Kα1 radiation source, λ=1.540598 Å, 45kV, 40mA, an incidence angle of 1° and a step of 0.005 degrees per second. XRD patterns were analyzed with High Score Plus software and Rietveld refinement, so that the proportion of presented phases in the coating and the crystallite size were calculated. Amorphous phases existing in the coatings were determined by a Horiba Jobin Yvon Labram high resolution Microraman using a Helium-Neon laser beam with wavelength of 633nm and 17mW, and using data obtained from the Software Labspec. The average surface roughness (Ra) of the coated samples, resulting from three measurements, was determined with an Atomic force microscope (AFM) Easyscan 2 Flex simple stage in contact mode using a silicon nitride tip. The hardness of the uncoated and coated steel samples was determined by knoop test method. For the measures a microindenter Shimadzu model HMV-G20 and a load of 25 grf were used according to the norm ASTM C1326 – 13. The hardness of each sample was calculated of the average value of 9 measurements. The friction coefficient and wear rate were evaluated in triplicate by a "ball on disc" tribometer, using a 6mm diameter alumina counter ball, 2mm radius wear track, sliding distance of 17.60 m and under 3N normal load, according with ASTM G99-95 norm. The loss of mass during the test was determined by weighing the samples before and after the test with a precision balance Mattler Toledo UMX5 comparator, with four digit decimal. All experiments were realized at a temperature (19 ±2)°C and relative humidity (48.5 ±2) %; the samples for this study were previously washed in ultrasonic bath with ethanol and then dried. The wear rate was determined by mean of **Equation 1:**

Figure 1. Cross section SEM micrographs of TaN deposited on steel samples with different nitrogen gas flow content: a) 12%, b) 14%, c) 20% and d) 25%.

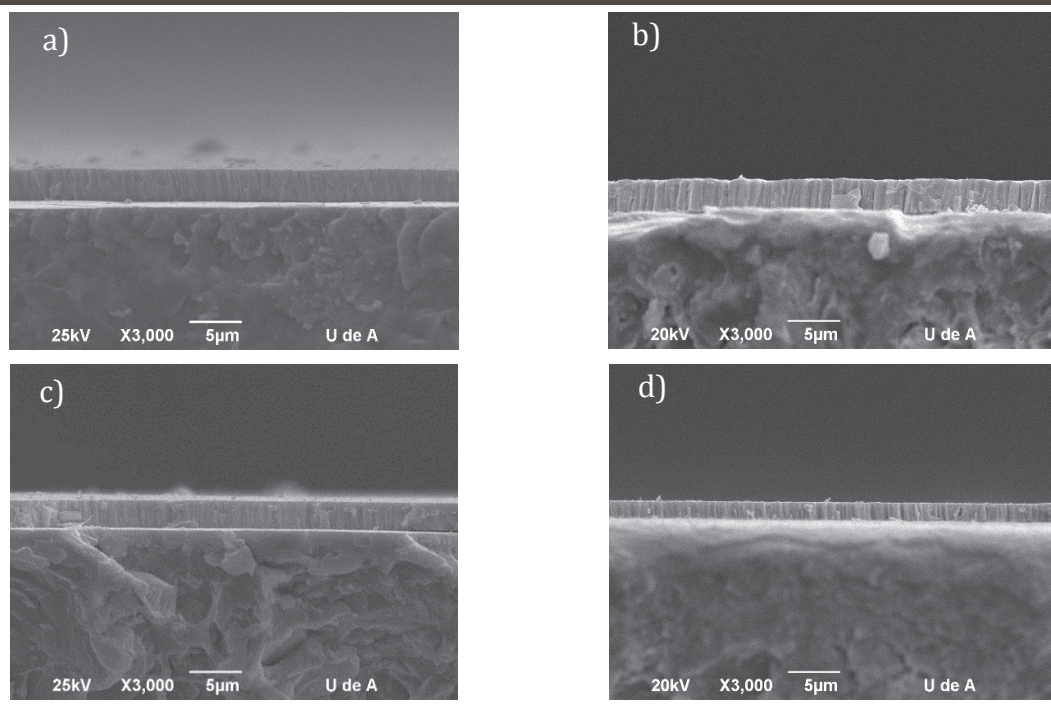

$$K = \frac{M}{F.s} \quad (1)$$

Where:

K: is a wear rate (Kg/Nm)

M: mass lost in the essay (Kg)

F: applied load (N)

s: sliding distance (m)

Additionally, the wear tracks were analyzed by scanning electron microscope (SEM), in order to elucidate the possible wear mechanisms'.

3. RESULTS AND DISCUSSION

3.1. Coating morphology and chemical composition.

Figure 1 shows the cross section SEM micrographs of TaN coatings for different nitrogen contents. These micrographs showed a homogenous microstructure of the coatings and columnar grain growth perpendicular to the substrate's surface with possible nano-scaled voids presented between the columns and at the grain boundaries following the Thornton growth model (Thornton 1974).

Figure 2. SEM surface images and EDX spectra of TaN coatings for two nitrogen contents: a) TaN-1, b) TaN- 4, c) TaN-5.

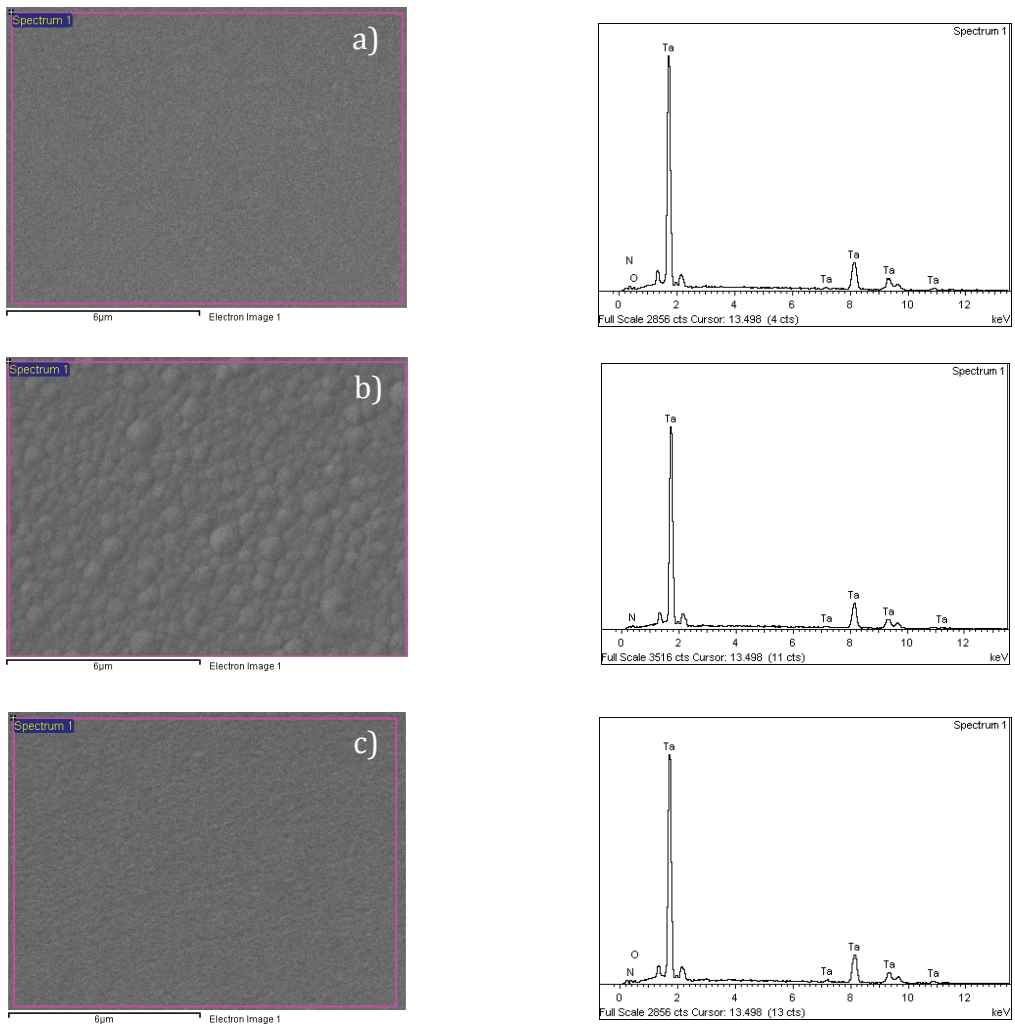

It was observed that the higher the nitrogen gas flow content, the more compact and defined columns of the coatings. In the same way, the coating thickness (measure in triplicate) decreases, as shown in **Table 2**. The elemental chemical composition of the TaN coatings, as determined by EDX, is consigned in **Table 2**. The percentage content of the elements for each sample was the average of three measurements. Due to the low resolution of ESD technique for determining the elemental chemical composition of elements such as N, C and B, among others, the atomic percentage of nitrogen in the coatings resulted from the difference of the Ta- content of 100%. Thus the nitrogen content in the coatings increased slowly with the increment of N_2 gas flow in the Ar/N2 gas mixture, while the atomic percent of tantalum decreased. The thickness decrease is associated with the increase of nitrogen in the system gases mixture, which displaces the argon partial volume, decreasing the pulverization rate of Ta target as well as the deposition rate of the coatings on the substrate. Another reason for a decrease of the target sputtering rate is the formation of a compound layer on the Ta cathode (target poisoning). The low sputtering rate of the Ta target with higher nitrogen content, and therefore, the reduction of deposition rate of TaN on the substrate, allows tantalum ions and atoms better rearrangement on the substrate surface over the time.

Figure. 3. AFM surface images and line profiles of TaN coatings for two nitrogen contents: a) TaN-1, b) TaN-4.

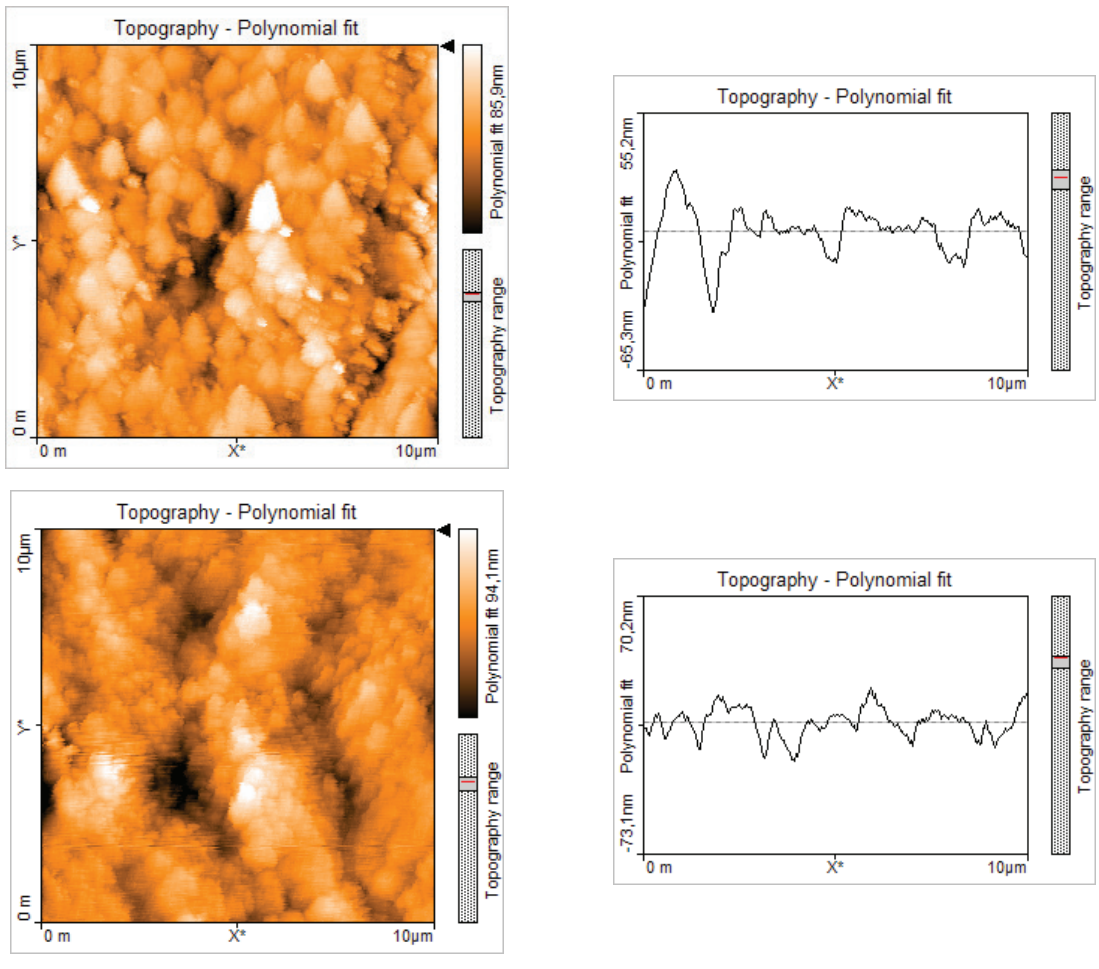

TABLE 2. TaN COATINGS DEPOSITED ON SILICON SUBSTRATES: ATOMIC COMPOSITION, THICKNESS, ROUGHNESS, AND CRYSTALLITE SIZE.

Sample	Composition (Atomic %)		Thickness (μm)	Roughness (nm)	Crystallite size (nm)
	Ta	**N**			
TaN- 1	53.7	46.3	3.3±0.06	9.4±1.12	8.6±0.013
TaN- 2	53.3	46.7	3.6±0.07	79.6±9.60	6.1±0.070
TaN- 3	49.6	50.4	2.2±0.04	12.7±1.52	1.9±0.024
TaN- 4	49.0	51.0	2.1±0.04	10.6±1.27	7.4±0.083
TaN- 5	47.7	52.3	1.8±0.36	35.0±4.20	12.5±0.014

This allows greater grain stacking, increasing the coating density and decreasing its thickness additionally. Moreover, by increasing the nitrogen content in the coatings, it occupies continuously the lattice's interstices of the TaN generating distortion of its lattice and also leading to a densification of the microstructure and probably to a grain refinement. Similar features were observed by S. Tsukimotoet. Al. (Tsukimoto *et al*. 2004) for the deposition and growth of the TaN coatings.

The top SEM view micrographs and resulting spectra of the chemical composition of the coated silicon samples TaN-2 and TaN-4 measured by EDX are shown in **Figure 2**. This micrographs show an apparently grain refinement when nitrogen content increases, according to the preceding discussion about **Figure 1**, where the grain boundaries practically disappear for nitrogen contents of 25%, also indicating an increase of the amorphicity degree of the coatings as it will be discussed below. The grain size could not be measured because the used AFM did not have the necessary resolution and provided much background noise.

In **Figure 3** are observed the surface topographies of the coated samples TaN-1 and TaN-4 obtained by AFM including their respective linear profiles by means of which the average surface roughness value of 3 measurements was determined, as shown in **Table 2**. In both images, it can see that the grains consist of fine crystallites packaged in clusters similar to a bunch of grapes. Such structures were also reported by Yang, J.J. *et al* (Yang *et al*. 2014).

Except for the sample TaN-2 grown with N_2 14%, the remaining coatings had a similar roughness near to 10nm. However, the roughness increases again above 20% of nitrogen contents, which can be associated with the excessive amorphous phase formation of TaN identified in the XRD patterns and Microraman spectra, which will be discussed later. It is important to note, that the roughness and the preferential growth orientation of certain phases in the coatings deposited on silicon, may vary if a substrate of polycrystalline steel 420 is used, due to the low roughness and mono-crystallinity of silicon.

3.2. Coatings phases composition

X-ray diffraction patterns of TaN coatings for different nitrogen content added to the N2/Ar gas mixture are shown in **Figure 4**. All coatings show characteristic peaks of cubic TaN, specifically fcc (111) (International Center for Diffraction Data 1997), (200) (International Center for Diffration Data 1997) and bcc (220) structures. TaN (111) peak decreases when nitrogen flux increases, and disappear almost completely above 14% N_2 content in the coating. Conversely, cubic TaN peak (200) becomes more intense as the nitrogen content increases, but above 18% N_2, the peak decreases again and become wider. This behavior suggests a tendency to structure amorphicity that is accompanied with the formation of the hexagonal phase Ta_5N_6 at 38° for samples coated with 14% and 18% N_2. Consequently, the sample coated with 25% N_2 presents a large amorphous zone between 30° and 35° and between 45° and 55°, where Ta_4N_5 and other nitrogen rich amorphous TaN phases appear, generating wide peaks of the TaN (220) cubic phase, and fundamentally of TaN (200) phase. A possible explanation for the change in the orientation of TaN (111) to TaN (200) with the increase of nitrogen content, is that the TaN (TaN-3 and TaN-4) phases are closer to Ta/N=1 stoichiometry corresponding to the most thermodynamically stable system and favoring the

TaN (200) phase formation with the smallest growth energy(Moura *et al*. 2011).

Figure 4. X- ray diffraction patterns of TaN films deposited on Si (100) at various N2 percentages.

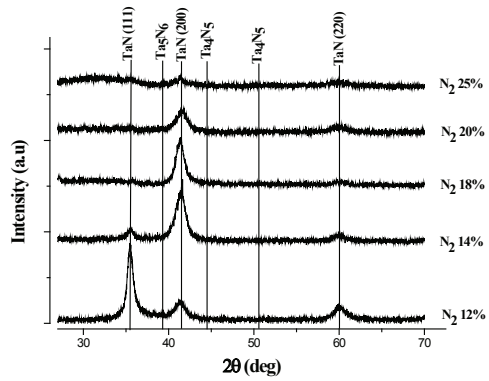

In order to identify and quantify the present phases in the different coatings of TaN, HighScore Plus software was used, performing Rietveld refinement in diffraction patterns. The resulting phases in each coating are shown in **Figure 5**, and it can be seen a decrease of the cubic TaN, and the beginning of the formation of the Ta_5N_6 and Ta_4N_5 phases, both with amorphous character, when the nitrogen content increases. The Ta_4N_5 phase is significantly increased in the coatings with nitrogen percentages higher than 18%. Finally in the TaN-5 coating, the high content of Ta_4N_5 and the appearance of the substoichiometric $Ta_{0.83}Na$ and $TaN_{0.9}$ phases suggest that this coating has a amorphous structure. Using Rietveld refinement, the crystallites size of TaN coatings for different nitrogen contents was determined, as shown in **Table 3**. An example of such calculation is shown here for TaN-1 coating, which presents in its main peak localized at 35.48° a 8.6 nm crystallite average size, and for TaN-4 coating with a crystallite size lower than 7.4 nm at its main peak localized at 41.24°. According to **Figure 5** the TaN-4 sample contents 79.4% of amorphous Ta_4N_5 phase, whose average crystallite size is 1.1nm, that leads to a reduced average crystallite size of this coated sample compared to that of TaN-1. The above discussed is corroborated with the average full width at the half maximum of the peak FWHM [°2θ] by 0.81, 1.59 for the phases of TaN (200) in TaN-1 and TaN-4 respectively, and 3.91 for Ta_4N_5 phase in TaN-4coating.

Figure 5. TaN phases present in films deposited on Si (100) at various N2 contents determined by HighScore Plus software (TaN- reference pattern 98-018-0957 / 98-064-4704 ICSD, Ta5N6 reference pattern 98-016-6512 ICSD, Ta4N5 reference pattern 98-002-9328 ICSD).

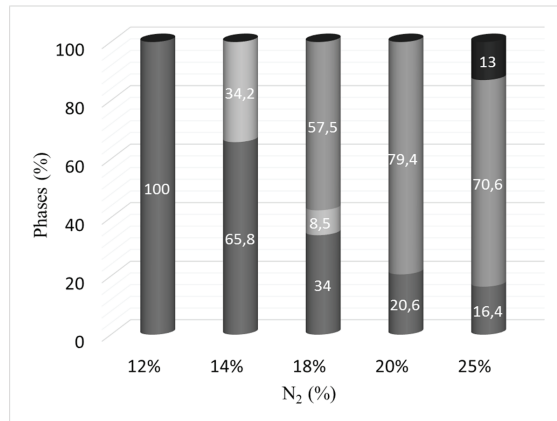

It should be noted that the FWHM is inversely proportional to the crystallite size and is consistent with the previous analysis. To complement the XRD-evaluation of the existing phases in the coatings of TaN, and especially to support the possible existence of amorphous phases, a Microraman spectroscopy characterization of them were carried out. **Figure 6** shows the Microraman patterns obtained for TaN with different N_2 contents. The peak between 60 and 190 cm^{-1} is assigned to a longitudinal acoustic (LA) mode, while two wide peaks between 390 and 800 cm^{-1} are related to a first-order acoustic (A-O) and optical (O) mode, respectively. The latest associated with the presence of point defects in the structure of TaN and indicating the presence of amorphous phases in the coatings. The small peak observed at 250 cm^{-1} for the TaN-1 sample it´s not reported in the literature when the stoichiometric value of nitrogen is less than 1.37 and is associated to a N-rich TaN phase (Spyropoulos-Antonakakis *et al*. 2013). With increasing nitrogen content the intensity

of the peak between 390 and 800 cm^{-1} decrease indicating a reduction of the coating's crystallinity. This behavior is related to an increase of disorder, of Ta- vacancies and N sites on sublattices, that further conduce to a shift of the peak centered at 111.8 cm^{-1} towards lower values of wave length for the samples TaN-4 and TN-5 indicating the occurrence of substoichiometric TaN- phases poor in nitrogen, similar results were obtained by (Spyropoulos-Antonakakis *et al*. 2013; Lima *et al*. 2012; Stoehr *et al*. 2011). The above observations are consistent with the results discussed by the above X-ray diffraction measurements. These findings are also consistent with the results of H.B. Nie *et al.* (Nie *et al*. 2001) who demonstrated through HRTEM analyses that the TaN coatings deposited by magnetron sputtering with high nitrogen contents, present small crystalline domains embedded in an amorphous matrix.

Figure 6. Microraman patterns of TaN films deposited on Si (100) at various N2 contents.

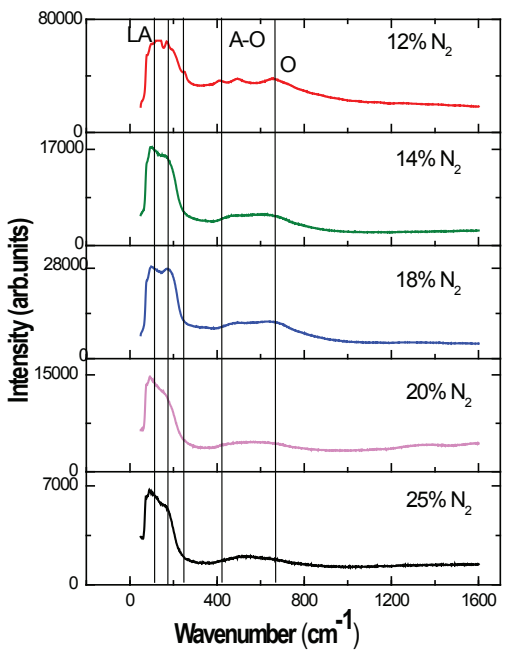

3.3. Mechanical and tribological properties

3.3.1 Hardness

The hardness of the coated steel samples was determined by Knoop indentation method applying a low load of 250 mN to minimize the influence of the substrate on the coating's hardness. As shown in **Figure 7** the nitrided 420 steel sample exhibited a hardness of 5.2 GPa higher than the hardness of the untreated sample of 3.4 GPa. In general terms, the hardness of the coated steel samples decreased with increasing N_2 contents in the coatings, this may be associate, firstly, with the effect of the hardness of the substrate since the thickness decreases with the nitrogen content, and on the other hand, with the increasing formation of nitrogen rich amorphous phases, as determined and described by the XRD and Microraman evaluation. The highest hardness of 21.3 GPa was obtained for the TaN-1 sample due probably to its high crystallinity and elevated content of the cubic fcc phases. The relative low hardness of 12.8 GPa for the TaN-2 sample is possible associated to the formation of the hexagonal Ta_5N_6 phase as discussed by the **Figure 5**.

Figure 7. Hardness of the untreated, nitrided and with TaN coated AISI 420 steel samples.

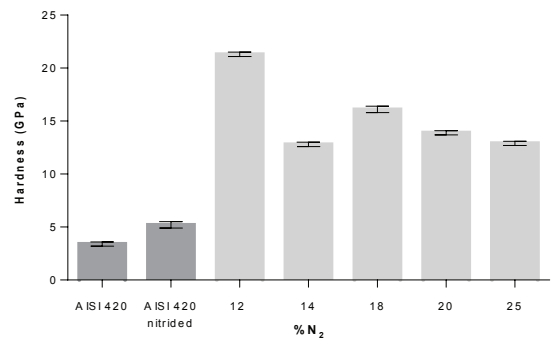

3.3.2 Wear rate and friction coefficient

Figure 8 compare the friction coefficient and wear rates values of uncoated and with TaN coated steel samples for different nitrogen gas flow contents

in the Ar/N_2- gas mixture. From all coated samples, the sample TaN-1 presented the lowest wear rate, due to its cubic fcc microstructure, highest hardness and lowest friction coefficient. TaN-2 coating exhibited the highest wear rate, which is probably associated with its high content of the hexagonal phase Ta_5N_6 as well as with its high roughness, low hardness and high friction coefficient. The TaN-1 sample showed a wear coefficient 40 times lower than the uncoated 420 steel sample indicating a promising application of TaN for wear protective coatings.

Tracks wear to TaN-1 and TaN-2, corresponding to the best and worst tribological behavior respectively are shown in **Figure 9**. In **Figure 9a**, the TaN-1 coating track shown an accumulation of material on the inner edge of the sliding track, and some debris in the middle which were agglomerated and have suffered plastic deformation in contact with the alumina counterbody. Regarding to TaN-2 in **Figure 9b**, the coating has been removed entirely in some areas of the wear track, and can be found several delamination sites, which were evident in the inner and outer edges; this response seem to be correlated with the highest roughness, coinciding with studies realized by J. Takadoum and H. Houmid Bennani, who gave insights on the influence of thickness and roughness coatings in the tribological behavior (Takadoum & Bennani 1997). All coatings suffered adhesive wear mechanisms, due to micro soldering in some points of contact as a result of relative movement generated in the test.

Figure 8. Friction coefficient and wear rate of the untreated and with TaN coated 420 steel samples for different N_2 contents.

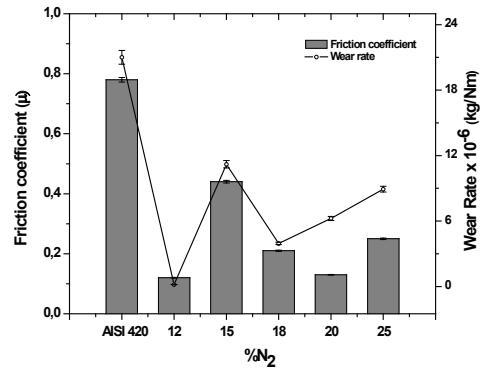

Figure 9. Wear tracks EDX mappings for the coatings for two nitrogen contents: a) TaN-1, b) TaN-2.

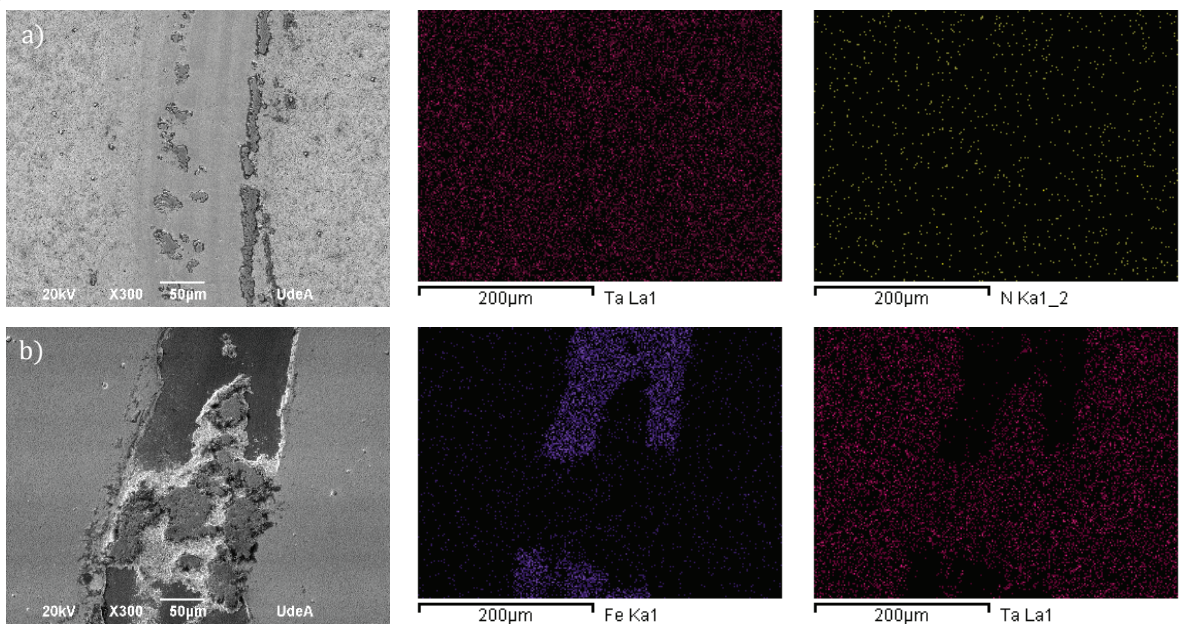

4. CONCLUSIONS

The nitrogen content in the work gas mixture has a strong influence on the elemental chemical and phase composition, microstructure, and surface topography of the coatings, which could be established in this work.

When the nitrogen content increase in the TaN coatings leads to a reduction of roughness, grain size, and coating thickness, which is probably associated with the process of nucleation and growth of the coating and with the lattice distortion generated by the diffusion von nitrogen atoms to the interstices of the cubic TaN structure, as well as with the reduction of the sputtering rate of the Ta-target, that mainly negative influence the deposition rate of TaN on the substrates.

At low nitrogen content TaN possess a crystalline cubic structure with preferential growth orientation in the (111) and (200) planes, that strongly changes to the (200) plane accompanied by the formation of the hexagonal Ta_5N_6 phase for the TaN-2 and TaN-3 reducing simultaneously the coatings hardness and wear resistance. Above 18% nitrogen contents in the TaN- coatings, all peaks become wider and appear other nitrogen rich phases suggesting a tendency to structure amorphicity, as could be observed by XRD and Microraman analysis. The obtained and discussed results of this work represent an important data base for future researches and are helpful to select the appropriate parameter of the deposition process of TaN coatings for a given application.

ACKNOWLEDGMENTS

The authors are grateful to Universidad de Antioquia and to ''Departamento Administrativo de Ciencia, Tecnología e Innovación COLCIENCIAS'' for its financial support to the Project RC. No. 0940 – 2012,

REFERENCES

International Center for Diffraction Data, (1997). JCPDS-Joint Committee on Powder Diffraction Standards - File card N°32-1283.

International Center for Diffration Data, (1997). JCPDS-Joint Committee on Powder Diffraction Standards - File card N°39-1485.

Lima, L.P.B.; Diniz, J.A.; Doi, I.; Miyoshi, J.; Silva, A.R.; Godoy Fo, J.; Radtke, C. (2012). Oxygen incorporation and dipole variation in tantalum nitride film used as metal-gate electrode. *Journal of Vacuum Science & Technology B: Microelectronics and Nanometer Structures*, 30(4), p.042202. Available at: http://scitation.aip.org/content/avs/journal/jvstb/30/4/10.1116/1.4729599 [Accessed September 2, 2015].

Moura, C.; Constantin, D.G.; Munteanu, D. (2011). Structural , optical and decorative properties of TaNx thin films prepared by reactive magnetron sputtering. *Bulletin of the Transilvania University*, 4(2), pp. 59.

Nie, H.B.; Xu, S.Y.; Wang, S.J.; You, L.P.; Yang, Z.; Ong, C.K.; Li, J.; Liew, T.Y.F. (2001). Structural and electrical properties of tantalum nitride thin films fabricated by using reactive radio-frequency magnetron sputtering. *Applied Physics A Materials Science & Processing,* 73(2), pp. 229–236. Available at: http://link.springer.com/10.1007/s003390000691.

Pino, J., (2008). Estudio nanométrico de biocompatibilidad y adhesividad celular a biomateriales utilizados en cirugía ortopédica. Santiago de Compostela.

Riekkinena, T.; Molariusa, J.; Laurilab, T.; Nurmelaa, A.; Sunia, I.; Kivilahtib, J.K. (2002). Reactive sputter deposition and properties of TaxN thin films. *Microelectronic Engineering*, 64(1-4), pp. 289–297.

Spyropoulos-Antonakakis, N.; Sarantopoulou, E.; Drazic, G.; Kollia, Z.; Christofilos, D.; Kourouklis, G.; Palles, D.; Cefalas, A.C. (2013). Charge transport mechanisms and memory effects in amorphous TaNx thin films. *Nanoscale research letters*, 8(1), p.432. Available at: http://www.pubmedcentral.nih.gov/articlerender.fcgi?artid=4016540&tool=pmcentrez&rendertype=abstract.

Stoehr, M.; Shin, C.-S.; Petrov, I.; Greene, J. E. (2011). Raman scattering from TiNx ($0.67 \leq x \leq 1.00$) single crystals grown on MgO(001). *Journal of Applied Physics*, 110(8), pp.0–4.

Takadoum, J.; Bennani, H.H., (1997). Influence of substrate roughness and coating thickness on adhesion, friction and wear of TiN films. *Surface and Coatings Technology*, 96, pp. 272–282.

Thornton, J.A., (1974). Influence of apparatus geometry and deposition conditions on the structure and topography of thick sputtered coatings. *Journal of vacumm science & Tecnologhy*, 11, pp. 666–670.

Tsukimoto, S.; Moriyama, M.; Murakami, M. (2004). Microstructure of amorphous tantalum nitride thin films. *Thin Solid Films*, 460(1-2), pp.222–226. Available at: http://linkinghub.elsevier.com/retrieve/pii/S0040609004001257 [Accessed April 21, 2014].

Westergård, R.; Bromark, M.; Larsson, M.; Hedenqvist, P.; Hogmark, S. (1997). Mechanical and tribological characterization of DC magnetron sputtered tantalum nitride thin films. *Surface and Coatings Technology*, 97, pp. 779–784.

Yang, J.J.; Miao, F.M.; Tang, J.; Yang, Y.Y.; Liao, J.L.; Liu, N. (2014). Multi-scale kinetic surface roughening of reactive-sputtered TaN thin films characterized by wavelet transform approach. *Thin Solid Films*, 550, pp. 367–372. Available at: http://linkinghub.elsevier.com/retrieve/pii/S004060901301804X [Accessed June 3, 2014].

PARA CITAR ESTE ARTÍCULO / TO REFERENCE THIS ARTICLE / PARA CITAR ESTE ARTIGO /

Bejarano Gaitán, G.; Echavarría García, A.M.; Quirama Ossa, A.C.; Osorio Vélez, J.A. (2016). Deposition and Properties Characterisation of TaN Coatings Deposited at Different Nitrogen Contents. *Revista EIA*, 13(25), enero-junio, pp. 69-80. [Online]. Disponible en: DOI: http:/dx.doi.org/10.14508/reia.2016.13.25.69-80